Expansion of a Quantum Gas Released from an Optical Lattice

F. Gerbier,[1,*] S. Trotzky,[2] S. Fölling,[3] U. Schnorrberger,[2] J. D. Thompson,[2] A. Widera,[4] I. Bloch,[2] L. Pollet,[5] M. Troyer,[5] B. Capogrosso-Sansone,[6] N. V. Prokof'ev,[5,6,7] and B. V. Svistunov[6,7]

[1]*Laboratoire Kastler Brossel, ENS, UPMC, CNRS, 24 rue Lhomond, 75005 Paris, France*
[2]*Institut für Physik, Johannes Gutenberg-Universität, 55099 Mainz, Germany*
[3]*Department of Physics, Harvard University, Cambridge, Massachusetts 02138, USA*
[4]*Institut für Angewandte Physik, 53115 Bonn, Germany*
[5]*Theoretische Physik, ETH Zurich, 8093 Zurich, Switzerland*
[6]*Department of Physics, University of Massachusetts, Amherst, Massachusetts 01003, USA*
[7]*Russian Research Center "Kurchatov Institute," 123182 Moscow, Russia*

(Received 26 July 2008; published 9 October 2008)

We analyze the interference pattern produced by ultracold atoms released from an optical lattice, commonly interpreted as the momentum distributions of the trapped quantum gas. We show that for finite times of flight the resulting density distribution can, however, be significantly altered, similar to a near-field diffraction regime in optics. We illustrate our findings with a simple model and realistic quantum Monte Carlo simulations for bosonic atoms and compare the latter to experiments.

DOI: 10.1103/PhysRevLett.101.155303 PACS numbers: 67.85.−d, 03.75.Gg, 03.75.Hh, 05.30.Jp

Experiments with ultracold quantum gases in optical lattices rely heavily on time-of-flight (ToF) expansion to probe the spatial coherence properties of the trapped gas [1–8]. When the phase coherence length is large compared to the lattice spacing, the postexpansion density distribution shows a sharp interference pattern with the same symmetry as the reciprocal lattice. As the phase coherence length decreases, e.g., on approaching the Mott insulator (MI) transition, the visibility of this interference pattern decreases accordingly [1]. To obtain a more precise understanding beyond this qualitative description, it is usually assumed that the density distribution $n_{\mathrm{ToF}}(\mathbf{r})$ of freely expanding clouds provides a faithful map of the initial momentum distribution.

In this Letter, we point out that, in general, the ToF distribution differs from the momentum distribution for a finite time of flight, the latter being recovered only in the "far-field" limit $t \to \infty$. Practically, the ToF and momentum distributions become identical after a characteristic expansion time $t_{\mathrm{FF}} = mR_0 l_c/\hbar$, which depends on the particle mass m, the coherence length l_c, and the cloud size R_0 prior to expansion. This time scale can be understood in analogy with the diffraction of a coherent optical wave by a periodic grating. Then the characteristic t_{FF} in the expansion problem exactly corresponds to the Fresnel distance in the diffraction problem. The far-field regime is typically reached when the coherence length is short, for example, for a cloud in the MI regime or a thermal gas well above the critical temperature. We show that, for phase-coherent samples where a sizable fraction of the atoms are Bose condensed, the far-field condition is usually not met for typical expansion times used in current experiments [1–8]. Experimental measurements and quantum Monte Carlo simulations are used to demonstrate that this results in substantial changes in the ToF distribution. We also discuss implications for the interpretation of the ToF images.

We consider an ultracold boson cloud released from a periodic trapping potential with cubic symmetry, lattice spacing $d = \lambda_{\mathrm{L}}/2$, and lattice depth V_0 given in units of the single-photon recoil energy $E_{\mathrm{R}} = h^2/2m\lambda_{\mathrm{L}}^2$, where λ_{L} is the lattice laser wavelength. In addition to the lattice potential, an "external" harmonic potential is present, due to both the magnetic trap and the optical confinement provided by the Gaussian-shaped lattice beams [4,9]. This external potential is responsible for the appearance of a shell structure of alternating MI and superfluid regions in the strongly interacting regime.

The density distribution after expansion for a time t is usually expressed as a product (see, e.g., [10])

$$n_{\mathrm{ToF}}(\mathbf{r}) = \left(\frac{m}{\hbar t}\right)^3 |\tilde{w}_0(\mathbf{k})|^2 \mathcal{S}(\mathbf{k}), \quad \text{with } \mathbf{k} = \frac{m\mathbf{r}}{\hbar t}, \tag{1}$$

where an envelope function $\tilde{w}_0$ is the Fourier transform of the on-site Wannier function w_0 and the interference term is

$$\mathcal{S}(\mathbf{k}) = \sum_{r_\mu, r_\nu} e^{i\mathbf{k}\cdot(\mathbf{r}_\mu - \mathbf{r}_\nu)} \langle \hat{a}_\mu^\dagger \hat{a}_\nu \rangle. \tag{2}$$

Here the operator $\hat{a}_\mu^\dagger$ creates an atom at site $\mathbf{r}_\mu$. To assess the validity of the far-field approximation used in Eq. (1), we quickly outline its derivation. Neglecting interactions during expansion (see below), the atomic field operator can be expressed in Schrödinger's picture as $\hat{\Psi}(\mathbf{r}, t) = \sum_{r_\nu} W_\nu(\mathbf{r}, t)\hat{a}_\nu$, where $W_\nu(\mathbf{r}, t = 0) = w_0(\mathbf{r} - \mathbf{r}_\nu)$. After the cloud is released, the wave function W_ν evolves in free flight as $W_\nu(\mathbf{r}, t) \approx (\frac{m}{\hbar t})^{3/2} \tilde{w}_0(\frac{m(\mathbf{r}-\mathbf{r}_\nu)}{\hbar t}) e^{i[m(\mathbf{r}-\mathbf{r}_\nu)^2/2\hbar t]}$ for $\omega_L t \gg 1$, with ω_L the oscillation frequency at the bottom of a lattice well. In the limit $t \to \infty$, the dependence on the initial site position $\mathbf{r}_\nu$ vanishes, and one recovers Eq. (1). For finite t, this dependence can be neglected in the envelope function [11] but not in the phase factor. We thus

obtain a generalized interference term

$$S_t(\mathbf{k}) = \sum_{r_\mu, r_\nu} e^{i\mathbf{k}\cdot(\mathbf{r}_\mu - \mathbf{r}_\nu) - i(m/2\hbar t)(\mathbf{r}_\mu^2 - \mathbf{r}_\nu^2)} \langle \hat{a}_\mu^\dagger \hat{a}_\nu \rangle. \quad (3)$$

Note that experimentally one observes a column distribution integrated along the probe direction $S_\perp(\mathbf{k}_\perp) = \int dk_z |\tilde{w}(k_z)|^2 S_t(\mathbf{k})$. This is included in latter comparison with experiments, but in the following we base our discussion on Eq. (3) for simplicity.

A fruitful analogy can be made with the theory of optical diffraction. The formation of the interference pattern results from the interference of many spherical matter waves emitted from each lattice site, with phase relationships reflecting the initial quantum state of the boson gas. We can exploit this analogy further by defining the equivalent of a Fresnel distance usually introduced in the theory of optical diffraction to estimate the importance of the quadratic phase factor $\propto \mathbf{r}_\mu^2 - \mathbf{r}_\nu^2$. Because the correlation function $\langle \hat{a}_\mu^\dagger \hat{a}_\nu \rangle$ suppresses contributions from sites distant by more than the characteristic coherence length l_c, we can estimate the magnitude of the quadratic phase in Eq. (3) as $\frac{m}{2\hbar t}(\mathbf{r}_\mu^2 - \mathbf{r}_\nu^2) \sim \frac{m l_c^2}{2\hbar t}$ near the cloud center and $\sim \frac{m l_c R_0}{\hbar t}$ near the cloud edge. Here R_0 is the characteristic size of the cloud before expansion. The most restrictive condition to apply the far-field approximation thus reads $t \gg t_{\mathrm{FF}}$, with

$$t_{\mathrm{FF}} \approx \frac{m l_c R_0}{\hbar}. \quad (4)$$

As an example, for a ^{87}Rb condensate with $l_c \approx R_0 \approx 30d$ and a lattice spacing $d \approx 400$ nm, one finds $t_{\mathrm{FF}} \approx 100$ ms, much larger than typical expansion times $t \approx 20$ ms in experiments [12]. In contrast, a gas with short coherence length (e.g., in the MI regime), with $l_c \gtrsim d$, will enter the far-field regime after a few milliseconds. We stress that the quadratic Fresnel term is intrinsically nonlocal, as the dephasing between two particular points $\mathbf{r}_\mu$ and $\mathbf{r}_\nu$ depends not only on their relative separation but also on their absolute positions. Although this has little effect deep in the superfluid or in the MI phase, this casts serious doubts on the validity of a local density approximation to compute quantitatively the ToF distribution in regimes where the coherence length is intermediate between the cloud radius and the lattice spacing.

To illustrate the influence of Fresnel terms on the interference pattern, we consider a 1D lattice with uniform phase and parabolic distribution of the occupation numbers $\langle \hat{a}_\mu^\dagger \hat{a}_\nu \rangle = c_\mu c_\nu$, with $c_\mu = \sqrt{1 - (\mu/N_{\mathrm{TF}})^2}$. The ToF distribution is given by

$$S_t(\tilde{k}) = \frac{1}{(2N_{\mathrm{TF}} + 1)^2} \left| \sum_{l=-N_{\mathrm{TF}}}^{N_{\mathrm{TF}}} c_l e^{i\tilde{k}l - i\beta^2 l^2/2} \right|^2, \quad (5)$$

with $\tilde{k} = kd$, $N_{\mathrm{TF}} = R_0/d = 30$ the Thomas-Fermi condensate size in lattice units, and where $\beta = \sqrt{md^2/\hbar t}$. The normalization factor $(2N_{\mathrm{TF}} + 1)^2$ would give the peak amplitude if the filling factor were uniform. We plot in Fig. 1(a) the distributions corresponding to $t = 20$ ms $\sim 0.2 t_{\mathrm{FF}}$ which shows a significant broadening of the distribution for a short time of flight when compared to the asymptotic result. For longer expansion times $t \sim t_{\mathrm{FF}} \sim 100$ ms, the far-field approximation is recovered to a good approximation.

Qualitatively, we expect from dimensional arguments that the peak width scales as $(\beta N_{\mathrm{TF}})^2 = t_{\mathrm{FF}}/t$ in the near field while approaching a constant value in the far field. The peak height thus increases as $(t/t_{\mathrm{FF}})^{\mathcal{D}}$ in $\mathcal{D}$ dimensions. This is confirmed by the one-dimensional calculation shown in Fig. 1(b). This dependence provides a means to check the importance of near-field effects experimentally. For the measurement, a sample of roughly 10^5 ^{87}Rb atoms has been prepared in a three-dimensional optical lattice with a depth $V_y = 6E_{\mathrm{R}}$ and subsequently released for expansion [14]. After recording a series of absorption images for different expansion times, the width of the interference peaks was extracted using a Gaussian fit to the images. We plot the results in Fig. 1(c), normalized to the separation between two diffraction peaks for convenience. The data confirm the t_{FF}/t scaling, indicating that

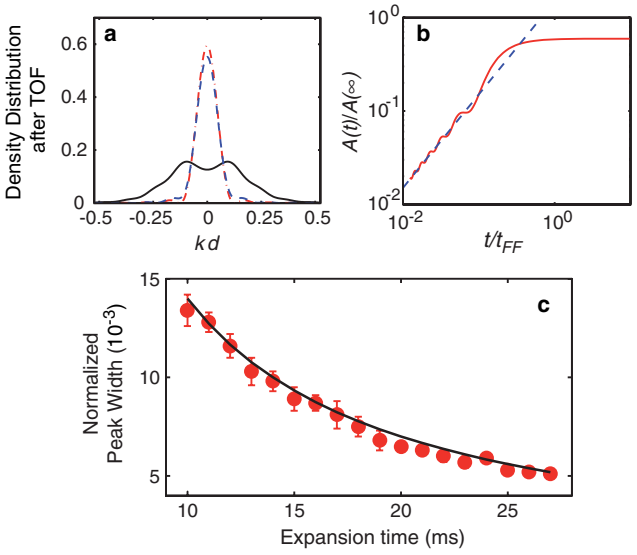

FIG. 1 (color online). (a) Momentum distributions for a one-dimensional lattice with parabolic distribution of the occupation numbers calculated using Eq. (5) (solid line: expansion time $t = 20$ ms; dashed line: expansion time $t = 100$ ms; dotted-dashed line: expansion time $t \to \infty$). (b) Evolution of the peak amplitude A with expansion time t/t_{FF}. The dashed line shows the expected near-field scaling in one dimension $A \propto t/t_{\mathrm{FF}}$. The number of sites is $2N_{\mathrm{TF}} + 1 = 61$ for (a) and (b). (c) Evolution of the width of the diffraction peaks with expansion time. The width has been normalized to the separation between two adjacent diffraction peaks for convenience. The circles show the experimental measurements and the solid line a fit by a hyperbola $\propto 1/t$, as expected in the near field.

the far-field asymptote is not reached even after the longest expansion time available in the experiment.

We now discuss briefly the effect of interactions on the expansion and show that this is negligible compared to the finite ToF effect. When the cloud has just been released from the lattice potential, each on-site wave function W_μ expands independently with a characteristic expansion time ω_L^{-1}, until $t \approx t^* = \sqrt{\hbar/(\omega_L E_R)}$ where the wave functions expanding from neighboring sites start to overlap. At this time, in the usual situation where $\omega_L t^* \gg 1$, the local density has dropped dramatically by a factor $(\omega_L t)^{-3} \ll 1$. Hence, the interaction energy converts into kinetic energy on the time scale of a few oscillation periods only, and expansion becomes rapidly ballistic. The parameter controlling the importance of interactions is given by $\eta = \frac{U}{\hbar\omega_L} \approx \sqrt{8\pi}\frac{a_s n_0}{\lambda_L}(\frac{V_0}{E_R})^{1/4}$, with U being the on-site interaction energy. For typical parameters, η is small (for instance, $\eta \approx 0.05$ for $V_0 = 10E_R$ and the experimental parameters of [3]). Hence, we expect only small corrections to the noninteracting picture of ballistic expansion. This has been confirmed using a variational model of the expanding condensate wave function [15]. This model predicts that the "Wannier" envelope expands faster as compared to the noninteracting case, which does not affect the interference pattern, and picks up a site-dependent phase factor formally similar to the Fresnel term discussed previously, but with a very weak prefactor $\eta \ll 1$ which has negligible influence in practice. We conclude that interactions essentially contribute to the expansion of the on-site wave functions, without significant dephasing of the interference pattern.

The discussion so far focused on fully phase-coherent systems, which only applies to the weakly interacting regime at low lattice depths. To investigate how the interference pattern is affected for strongly interacting systems (i.e., on approaching the Mott transition and beyond), we have performed large-scale three-dimensional quantum Monte Carlo (QMC) simulations accounting for the external trapping potential using the worm algorithm [16,17] in the implementation of Ref. [18]. The calculations were performed for $N = 8 \times 10^4$ atoms, using exactly the same parameters and system sizes (up to $\sim 200^3$) as in the experiments reported in Ref. [3]. The simulation was done at constant temperature $T = J/k_B$, where J is the hopping amplitude. This temperature is low enough to consider the system close to the ground state. Although simulations at constant entropy would be closer to the experimental situation, the temperature in the lattice was found to depend weakly on lattice depth in this parameter regime [19].

The ToF distributions calculated for finite and infinite expansion times are shown in Fig. 2. The simulations confirm explicitly the analysis made above: The interference pattern is strongly affected in the superfluid phase, and the effect becomes less and less pronounced as the lattice depth is increased and the Mott transition crossed. Note finally that the Fresnel phase suppresses the contribution from the edges of the cloud, thus favoring the contribution of the central region to the ToF pattern. This is especially important when superfluid rings surround a central MI region with lower coherence [20].

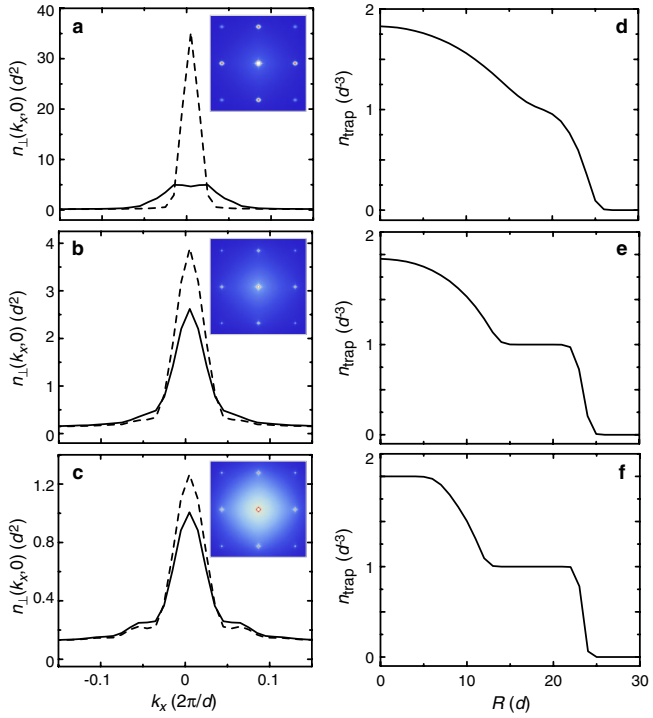

FIG. 2 (color online). Results from quantum Monte Carlo simulations. On the left column, we show a horizontal cut through the ToF distributions calculated using Eq. (3) for a finite expansion time $t = 14$ ms (solid line) compared to a cut through the profile calculated for $t \to \infty$ (dashed line). Units for $n_\perp$ are arbitrary. The insets show directly the two-dimensional ToF distributions for $t = 14$ ms. On the right column, we show the in-trap density profiles for reference. The lattice depths are $V_0 = 12E_R$ (a),(d), $15E_R$ (b),(e), and $17E_R$ (c),(f), respectively.

The interference pattern is often characterized by its visibility

$$\mathcal{V} = \frac{n_{\rm ToF}(\mathbf{k}_{\rm max}) - n_{\rm ToF}(\mathbf{k}_{\rm min})}{n_{\rm ToF}(\mathbf{k}_{\rm max}) + n_{\rm ToF}(\mathbf{k}_{\rm min})}, \tag{6}$$

with the choice $\mathbf{k}_{\rm max} d = (2\pi, 0)$ and $\mathbf{k}_{\rm min} d = \sqrt{2}(\pi, \pi)$ to cancel out the Wannier envelope in the division. We first evaluate the sensitivity of $\mathcal{V}$ to the Fresnel phase by plotting in Fig. 3 two theoretical "benchmark" curves assuming perfect experimental resolution (dashed and dotted-dashed lines for $t = 14$ ms and $t \to \infty$, respectively). We find little difference between the two curves when T/J is kept constant and small. Indeed, the Fresnel terms matter only for systems with a large coherence length, where the visibility is by construction very close to unity. We conclude that a detailed investigation of the superfluid side of the transition is better achieved by di-

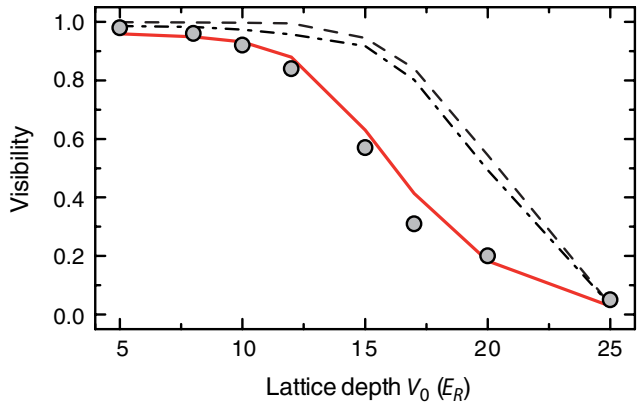

FIG. 3 (color online). Visibility of the interference pattern as defined in Eq. (6). The dashed and dotted-dashed lines show the quantum Monte Carlo result for infinite and finite ($t = 14$ ms) expansion times, assuming perfect experimental resolution. The solid line is computed for $t = 14$ ms accounting for finite experimental resolution. The simulations were performed at constant temperature $T = J/k_B$.

rectly measuring the ToF distributions, whereas the visibility is well-suited for short coherence lengths.

We also compare in Fig. 3 the experiments reported in Ref. [4] to the predictions of the QMC simulations (solid line). Here, we emphasize that, apart from the Fresnel terms, an accurate comparison requires one to account for the experimental resolution, which is limited by two effects. First, the signal was obtained by integration over a square box centered around the maxima or minima, the integration area being $\approx (0.11 \times 2\pi/d)^2$ in momentum units. This is comparable to a typical peak area, so that the visibility is calculated from the peak weight rather than from its amplitude. Second, the finite resolution of the imaging system (about 6 μm) is not negligible for the sharpest peaks. Accounting for these two effects when evaluating the QMC data, we find good agreement with the experimental results, although a fully quantitative comparison would require performing simulations and experiments at the same constant entropy. This entails that the experimental data are compatible with the system remaining at low enough temperatures (on the order of J/k_B) to cross a quantum-critical regime, in contrast to the analysis made in Refs. [21,22] which included neither near-field expansion nor experimental resolution.

In conclusion, we have analyzed the interference pattern observed in the expansion of a bosonic quantum gas released from an optical lattice. We showed that, due to an additional Fresnel-like phase appearing for a finite time of flight, the ToF distribution can be markedly different from the momentum distribution for clouds with large coherence lengths. Conversely, the visibility as calculated from Eq. (6) is rather insensitive to this effect. The Fresnel phase acts as a magnifying lens for the central region undergoing a Mott insulator transition by suppressing the contribution of the outer regions of the cloud when the central density is close to integer filling. This could eventually provide a way to investigate the physics near the quantum-critical point without "parasitic" contributions coming from coexisting superfluid rings.

Simulations were ran on the Brutus cluster at ETH Zurich. We acknowledge support from IFRAF, ANR (F. G.), DFG, EU, AFOSR (I. B.), the Swiss National Science Foundation (L. P.), NSF Grant No. PHY-0653183 (B. C. S., N. P., and B. S.), and DARPA (OLE project).

*fabrice.gerbier@lkb.ens.fr

[1] M. Greiner, O. Mandel, T. Esslinger, T. W. Hänsch, and I. Bloch, Nature (London) **415**, 39 (2002).
[2] T. Stöferle, H. Moritz, C. Schori, M. Köhl, and T. Esslinger, Phys. Rev. Lett. **92**, 130403 (2004).
[3] F. Gerbier, A. Widera, S. Fölling, O. Mandel, T. Gericke, and I. Bloch, Phys. Rev. Lett. **95**, 050404 (2005).
[4] F. Gerbier, A. Widera, S. Fölling, O. Mandel, T. Gericke, and I. Bloch, Phys. Rev. A **72**, 053606 (2005).
[5] S. Ospelkaus *et al.*, Phys. Rev. Lett. **96**, 180403 (2006).
[6] K. Günter, T. Stöferle, H. Moritz, M. Köhl, and T. Esslinger, Phys. Rev. Lett. **96**, 180402 (2006).
[7] I. B. Spielman, W. D. Phillips, and J. V. Porto, Phys. Rev. Lett. **98**, 080404 (2007).
[8] J. Catani, L. De Sarlo, G. Barontini, F. Minardi, and M. Inguscio, Phys. Rev. A **77**, 011603(R) (2008).
[9] M. Greiner, Ph.D. thesis, Ludwig-Maximilian University Munich, 2003.
[10] P. Pedri *et al.*, Phys. Rev. Lett. **87**, 220401 (2001).
[11] Replacing $\tilde{w}_0(k = \frac{m(\mathbf{r}-\mathbf{r}_\nu)}{\hbar t})$ by $\tilde{w}_0(k = \frac{m\mathbf{r}}{\hbar t})$ requires $t \gg R_0/d\omega_L$, $R_0/d\sqrt{\omega_L E_R/\hbar}$, or $t \gg 1$ ms for parameters as assumed in the text.
[12] This was independently established in Ref. [13], although the impact on the ToF distribution was not analyzed.
[13] E. Toth, A. M. Rey, and P. B. Blakie, Phys. Rev. A **78**, 013627 (2008).
[14] The experiment is similar to Ref. [1], expect for the wavelengths of the lattice beams used for the measurement in Fig. 1: $\lambda_x = 765$ nm for one axis x and $\lambda_{y,z} = 843$ nm for the other two. The lattice depths are chosen such that tunneling frequencies are equal.
[15] V. M. Pérez-Garcia, H. Michinel, J. I. Cirac, M. Lewenstein, and P. Zoller, Phys. Rev. Lett. **77**, 5320 (1996).
[16] N. V. Prokof'ev, B. V. Svistunov, and I. S. Tupitsyn, Zh. Eksp. Teor. Fiz. **114**, 570 (1998) [JETP **87**, 310 (1998)].
[17] N. V. Prokof'ev, B. V. Svistunov, and I. S. Tupitsyn, Phys. Lett. A **238**, 253 (1998).
[18] L. Pollet, K. V. Houcke, and S. M. A. Rombouts, J. Comput. Phys. **225**, 2249 (2007).
[19] L. Pollet, C. Kollath, K. V. Houcke, and M. Troyer, New J. Phys. **10**, 065001 (2008).
[20] G. G. Batrouni *et al.*, Phys. Rev. Lett. **89**, 117203 (2002).
[21] R. B. Diener, Q. Zhou, H. Zhai, and T.-L. Ho, Phys. Rev. Lett. **98**, 180404 (2007).
[22] Y. Kato, Q. Zhou, N. Kawashima, and N. Trivedi, Nature Phys. (in press).